Journal of Medicinal Chemistry Article

*J. Med. Chem.* **2010,** *53,* 6595–6602 **6595**
DOI: 10.1021/jm100345r

# 4-(3-Halo/amino-4,5-dimethoxyphenyl)-5-aryloxazoles and -*N*-methylimidazoles That Are Cytotoxic against Combretastatin A Resistant Tumor Cells and Vascular Disrupting in a Cisplatin Resistant Germ Cell Tumor Model

Rainer Schobert,*[,‡] Bernhard Biersack,[‡] Andrea Dietrich,[†] Katharina Effenberger,[‡] Sebastian Knauer,[‡] and Thomas Mueller*[,†]

[†]*Department of Internal Medicine IV, Oncology/Hematology, Martin Luther University Halle-Wittenberg, Ernst-Grube-Strasse 40, D-06120 Halle, Germany, and* [‡]*Organic Chemistry Laboratory, University Bayreuth, Universitätsstrasse 30, D-95440 Bayreuth, Germany*

*Received March 16, 2010*

New combretastatin A analogues featuring oxazole or *N*-methylimidazole bridged *Z*-alkenes and halo- or amino-substituted A-rings were tested against various cancer cell lines and in testicular germ cell tumor xenografts in mice. Imidazoles with 3-halo-4,5-dimethoxy substituted A-rings and 3-amino-4-methoxy substituted B-rings (**7b** and **8b**) were efficacious at nanomolar concentrations against cells of combretastatin A refractory HT-29 colon carcinoma, multidrug-resistant MCF-7/Topo breast carcinoma, and cisplatin-resistant 1411HP testicular germ cell tumor. They induced apoptosis and inhibited tubulin polymerization. While well tolerated by mice at high doses, these imidazoles initiated extensive intratumoral hemorrhage and regressions of highly vascularized 1411HP xenografts.

## Introduction

Combretastatin A-4 (Figure 1) was first isolated from the bark of the South African Cape Bushwillow (*Combretum caffrum*).[1] Fosbretabulin, its water-soluble phosphate prodrug, selectively damaged tumoral vasculature in clinical trials.[2] A drawback of combretastatin A-4 is its insufficient cytotoxicity which necessitates combination regimens with other drugs. A recent phase Ib trial revealed that combinations of fosbretabulin with carboplatin and paclitaxel were well tolerated and had antitumor activity in heavily pretreated patients with advanced cancer.[3] Treatment with combretastatin A-4 alone often led to the persistence of peripheral, quickly revascularizing cancer cells and hence to tumor relapses.[4] The related catechol combretastatin A-1 and its bisphosphate prodrug (OXi4503) are also strongly vascular disrupting[5,6] and led to tumor regressions especially when combined with other anticancer drugs such as bevacizumab[7] or doxorubicin.[8] Catechols are known to undergo redox cycling via quinoid intermediates, thus mediating the generation of reactive oxygen species and the alkylation of bionucleophiles.[6,9,10] Chemically stable derivatives of combretastatin A-4, which itself tends to isomerize to a biologically inactive *E*-alkene,[11−13] were obtained by incorporation of the *Z*-alkene in heterocycles such as imidazoles, oxazoles,[14] isoxazolines, pyridines, or triazoles.[4] For instance, imidazole **1** retains the tubulin affinity of the parent combretastatins while showing improved water solubility and pharmacokinetics. However, it is inferior to combretastatin A-4 with respect to cytotoxicity. The analogous highly cytotoxic oxazoles are hampered by unsatisfactory pharmacological properties.[11] In another study (3-halo-4,5-dimethoxyphenyl)stilbenes **2**, close analogues of combretastatin A-3, showed increased affinities for tubulin and a more selective activity profile against tumor cells including resistant ones. However, because of their insufficient water solubility, they require formulations as phosphate prodrugs in order to reach optimum uptake rates.[15] Fluorinated combretastatin derivatives were also synthesized by various other groups.[16−18] Herein we report new water-soluble, stable, and nontoxic oxazole and imidazole-bridged combretastatin derivatives with halo- or amino-substituted A-rings that show selective antitumoral activity in vitro and in vivo.

## Results and Discussion

**Chemistry.** The new imidazoles and oxazoles were prepared from the corresponding halo- and nitro-substituted *p*-toluenesulfonylmethyl isocyanides (TosMICs[a]). Commercially available 5-chloro- and 5-bromovanillin **3a**/**b** were reacted with iodomethane to give the veratraldehydes **4a**/**b**,[15] which were converted to the tosylmethylformamides **5a**/**b** by reaction with *p*-toluenesulfinic acid and formamide in the presence of camphorsulfonic acid (CSA). In the same way, 5-nitrovanillin as obtained by reaction of vanillin with fuming nitric acid in acetic acid was methylated to give veratraldehyde **4c**,[19,20] which was converted to formamide **5c**. Subsequently, the formamides **5** were dehydrated to the

*To whom correspondence should be addressed. For R.S.: phone/fax, +49 921 552679/1; e-mail, Rainer.Schobert@uni-bayreuth.de. For T.M.: phone/fax, +49 345 5577278/9; e-mail, thomas.mueller@medizin.uni-halle.de.

[a] Abbreviations: CAM, chorioallantoic membrane; CSA, camphorsulfonic acid; DME, 1,2-dimethoxyethane; DMF, *N*,*N*-dimethylformamide; MTT, 3-(4,5-dimethylthiazol-2-yl)-2,5-diphenyltetrazolium bromide; NBT, nitro blue tetrazolium; ROS, reactive oxygen species; SRB, sulforhodamine B; TBAI, tetrabutylammonium iodide; TosMIC, *p*-toluenesulfonylmethyl isocyanide; TUNEL, terminal deoxynucleotidyl transferase mediated dUTP nick end labeling.



Published on Web 08/23/2010

TosMIC derivatives **6** by treatment with phosphoroxychloride (Scheme 1).

The halo-substituted TosMIC derivatives **6a**/**b** were converted to *N*-methylimidazoles **7**/**8** by reaction with *N*-methylimines generated from the corresponding arylaldehydes (Scheme 2). Selective reduction of the nitro group of **7a**/**8a** with Zn/HCl gave the amines **7b**/**8b**. Treatment of the imidazoles **7b**–**d** and **8b**–**d** with 3 M HCl/dioxane afforded the respective water-soluble mono- or bis-hydrochlorides.

The nitro-substituted compounds **9a**–**e** were prepared likewise from the nitro-TosMIC derivative **6c** and the corresponding aldehydes and imines (Scheme 3). The amines **10a**–**d** were obtained by Pd-catalyzed transfer hydrogenation. The 3-chloroindole **9e** was reduced with Zn/HCl to amine **10e**. Finally, the compounds **10** were converted to water-soluble hydrochlorides.

**Biological Evaluation.** Figure 2 shows the growth inhibition in MTT assays of compounds **1**, **7b**, **8b**, **10a**, and **10e** in cells of the human tumor cell lines 518A2 melanoma, HL-60 leukemia, HT-29 colon carcinoma, KB-V1/Vbl cervix carcinoma, and MCF-7/Topo breast carcinoma. Table 1 summarizes the $IC_{50}$ (72 h) values as calculated from the

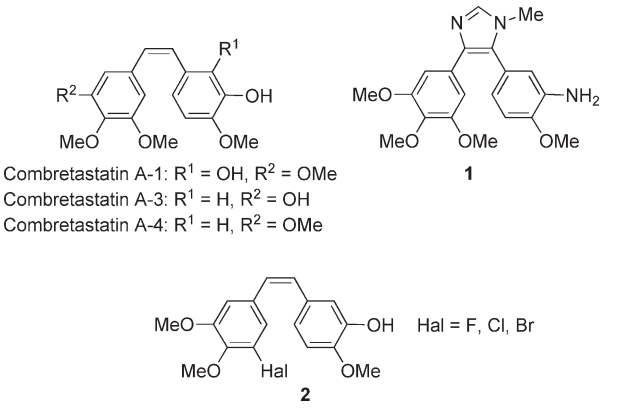


**Figure 1.** Combretastatins A-1, A-3, and A-4 and known analogues **1** and **2**: potent inhibitors of tubulin polymerization.

**Scheme 1.** Synthesis of TosMIC Derivatives **6**[a]

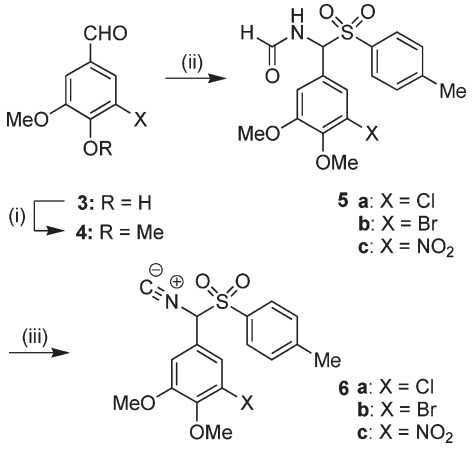


[a] Reagents and conditions: (i) MeI, $K_2CO_3$, TBAI, DMF, 24 h, room temp, 80–90%; (ii) $HCONH_2$, CSA, *p*-toluenesulfinic acid, 16 h, 60 °C, 51–58%; (iii) $POCl_3$, $Et_3N$, DME, 3 h, −5 °C, 57–74%.

**Scheme 3.** Synthesis of 4-(3-Aminoaryl)-Substituted Oxazoles and *N*-Methylimidazoles **10**[a]

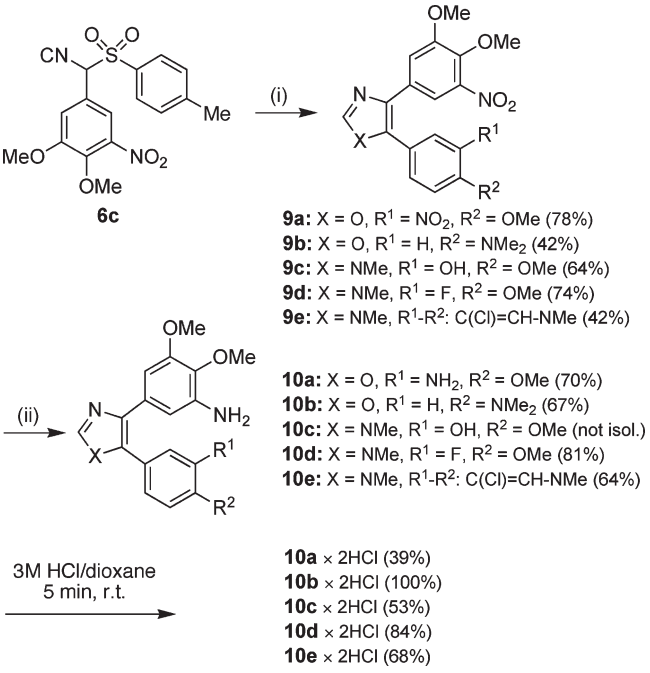


[a] Reagents and conditions: (i) ArCHO, $K_2CO_3$, DME/MeOH, 2 h, reflux, 42–86% (for X = O); ArCHO, $MeNH_2$ (33% in EtOH), AcOH, EtOH, 2 h, reflux (for X = NMe); then **6c**, $K_2CO_3$, DME/EtOH, 3 h, reflux, 64–74%; (ii) $HCO_2NH_4$, Pd/C (5%), MeOH, 2 h, reflux, 67–84% (for **10a**–**d**); Zn, HCl, THF, 10 min, room temp, 64% (for **10e**).

**Scheme 2.** Synthesis of 4-(3-Haloaryl)-Substituted *N*-Methylimidazoles **7** and **8**[a]

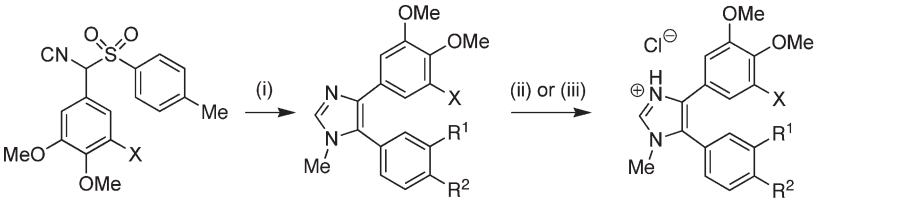


[a] Reagents and conditions: (i) ArCHO, $MeNH_2$ (33% in EtOH), AcOH, EtOH, 2 h, reflux; then **6a**/**b**, $K_2CO_3$, DME/EtOH, 3 h, reflux, 52–99%. (ii) For **7a** or **8a**: Zn, HCl, THF, 15 min, room temp, yield 40/91% (**7b**·2HCl/**8b**·2HCl). (iii) For **7c**,**d** or **8c**,**d**: 3 M HCl/dioxane, 15 min, room temp, 46–66%.

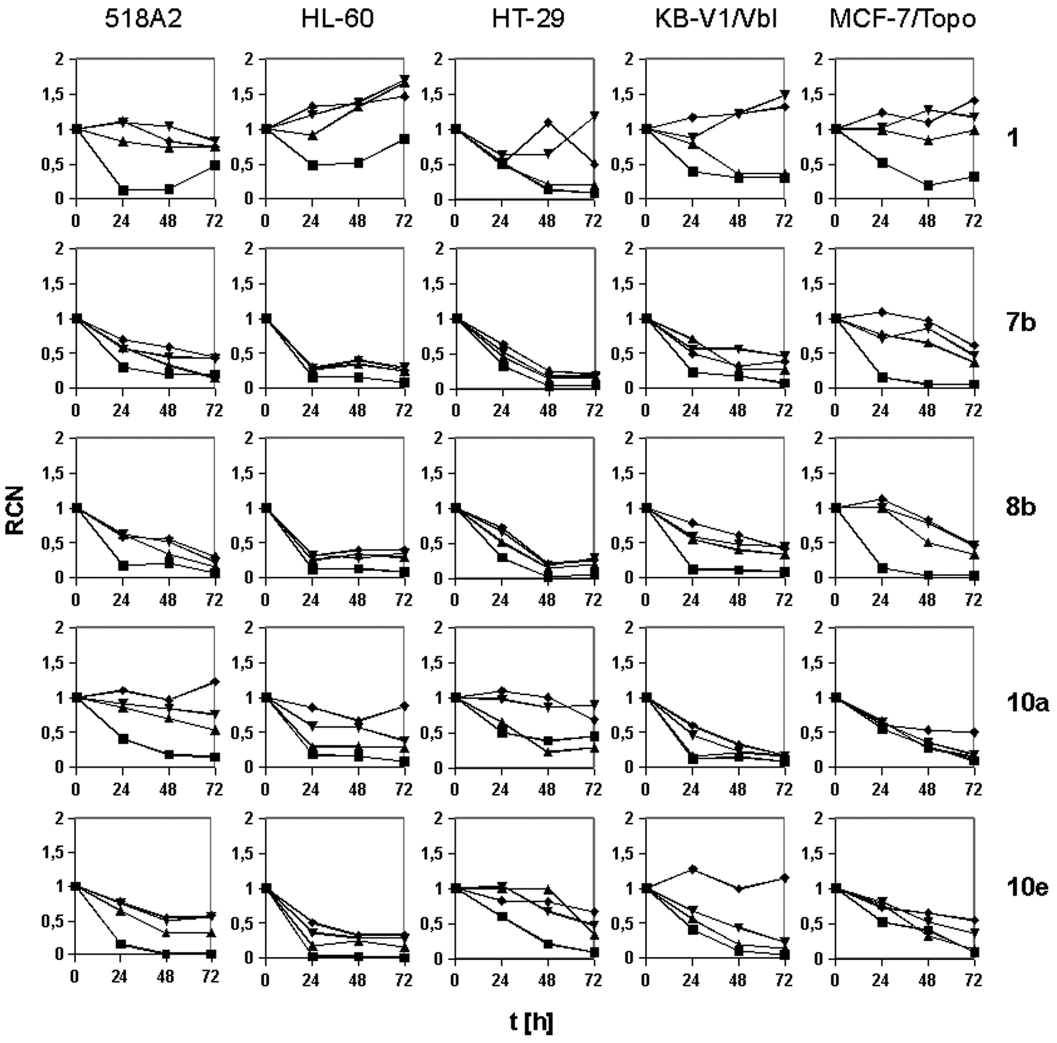


**Figure 2.** Cell growth inhibition by compounds **1**, **7b**, **8b**, **10a**, and **10e** at various concentrations (■, 100 $\mu$M; ▲, 1 $\mu$M; ▼, 0.01 $\mu$M; ◆, 0.001 $\mu$M) in cells of human 518A2 melanoma, HL-60 leukemia, HT-29 colon carcinoma, KB-V1/Vbl cervix carcinoma, and MCF-7/Topo breast carcinoma upon incubation for 24−72 h (*x*-axis). *Y*-Axis shows number of viable cells relative to untreated controls as ascertained by the MTT assay (RCN = relative cell numbers).

**Table 1.** Inhibitory Concentrations[a] ($IC_{50}$ [nM]) of Imidazoles **1**, **7**, **8**, **10c**−**e** and oxazoles **10a**,**b**, and Combretastatin A-4 (CA4) When Applied to Various Human Cancer Cell Lines

| | $IC_{50}$ (nM) for cell line | | | | | | |
|---|---|---|---|---|---|---|---|
| compd | 518A2 | HL-60 | HT-29 | KB-V1/Vbl | MCF-7/Topo | H12.1[b] | 1411HP[b] |
| **1** | > 100000 | > 100000 | 64 ± 14 | 300 ± 200 | > 10000 | *c* | *c* |
| **7b** | 62 ± 11 | 0.2 ± 0.05 | 0.06 ± 0.01 | 400 ± 170 | 320 ± 180 | ~ 30 | ~ 60 |
| **7c** | 400 ± 100 | > 10 000 | 530 ± 30 | *c* | *c* | *c* | *c* |
| **7d** | 2300 ± 200 | 0.02 ± 0.01 | 0.2 ± 0.1 | *c* | *c* | *c* | *c* |
| **8b** | 6.4 ± 1.4 | 0.1 ± 0.02 | 0.02 ± 0.01 | 200 ± 60 | 340 ± 160 | ~ 22 | ~ 54 |
| **8c** | 66 ± 16 | 9700 ± 300 | 510 ± 10 | *c* | *c* | *c* | *c* |
| **8d** | 860 ± 140 | 0.2 ± 0.01 | 4.3 ± 0.8 | *c* | *c* | *c* | *c* |
| **10a** | 2.0 ± 0.9 | 3.8 ± 1.2 | 57 ± 7 | 0.01 ± 0.01 | 1.23 ± 0.48 | *c* | *c* |
| **10b** | 110 ± 40 | 0.9 ± 0.1 | > 15 000 | *c* | *c* | *c* | *c* |
| **10c** | 2800 ± 300 | 4600 ± 400 | > 100 000 | *c* | *c* | *c* | *c* |
| **10d** | > 10000 | > 10 000 | > 50 000 | *c* | *c* | *c* | *c* |
| **10e** | 3100 ± 600 | 0.04 ± 0.02 | 14 ± 4 | 160 ± 60 | 3.8 ± 1.8 | *c* | *c* |
| CA4 | 18 ± 7 | 0.1 ± 0.0 | 3600 ± 140 | 0.4 ± 0.1 | 500 ± 200 | *c* | *c* |

[a] Values are derived from concentration-response curves (MTT, 72 h; Figure 2, S18) by applying the four-parameter Hill model. [b] SRB tests, 96 h (S19). $IC_{50}$ (96 h; cisplatin): ~400 nM (H12.1), ~3.5 $\mu$M (1411HP). [c] Not measured.

dose-response curves of Figure 2 according to the "four parameter Hill model". It also includes the $IC_{50}$ values for other analogous compounds and cell lines whose dose-response curves are depicted in the Supporting Information. The haloamino-substituted imidazoles **7b** and **8b** were distinctly more cytotoxic than the known reference compound **1** with $IC_{50}$ concentrations in the lower nanomolar range, even in the combretastatin A-4-resistant HT-29 and the multidrug-resistant

KB-V1 and MCF-7/Topo cells. The fluoro and *N*,*N*-dimethylaminoimidazoles **7c**/**8c** and **7d**/**8d** were generally less active than their amino congeners **7b**/**8b** (cf. Supporting Information).

The diamino substituted oxazole **10a** and imidazole **10e** were more efficacious at low concentrations than **1** and **7b**/**8b**

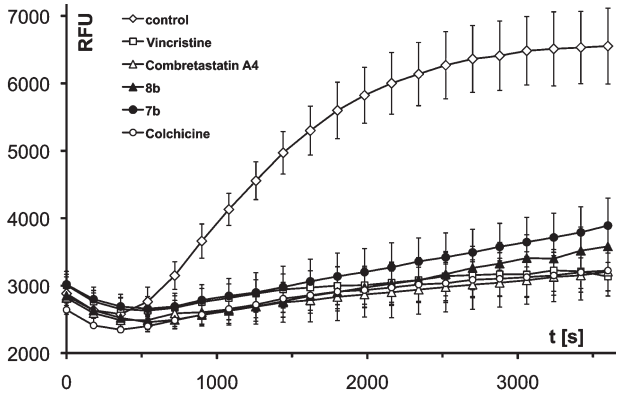


**Figure 3.** Effects of 3 $\mu$M each of compounds **7b**, **8b**, vincristine, colchicine, or combretastatin A-4 on the polymerization of tubulin as ascertained with a fluorescence-based assay kit from Cytoskeleton. Data are representative of four to five independent experiments. RFU = relative fluorescence units.

against both multidrug-resistant cells, i.e., KB-V1/Vbl and MCF-7/Topo. The reduced activity of compounds **10b**−**d** when compared to that of **10a** emphasizes the importance of the 3-amino group at the B-ring. The imidazoles **7b** and **8b** were also tested in vitro in a testicular germ cell tumor model comprising the highly chemosensitive cell line H12.1 and the cell line 1411HP, which is intrinsically resistant to cisplatin and other conventional chemotherapeutic drugs. These cell lines were chosen because they maintain their individual in vitro chemosensitivities to cisplatin when grown as xenograft tumors in mice.[21] Unlike cisplatin, imidazole **7b**/**8b** showed similar activity against the two germ cell tumor cell lines with $IC_{50}$(96 h) $\approx$ 20−60 nM (cf. Supporting Information). They also inhibited the polymerization of tubulin to a comparable extent when tested with the tubulin polymerization assay kit by Cytoskeleton. Figure 3 shows the time dependency of this process in samples containing **7b**, **8b**, or the reference compounds combretastatin A-4, colchicine, or vincristine.

In TUNEL assays, which allow the detection of apoptosis by labeling the 3′-OH ends of DNA fragments with fluorescein-tagged nucleotides, compounds **7b**, **8b**, and **10a** were found to induce death in HL-60 cells predominantly in an apoptotic way (~60% after 16 h of incubation with 10 $\mu$M drug). The extent of apoptosis-related mitochondrial damage in HL-60 cells was ascertained by means of the fluorescence dye JC-1 that detects changes in the mitochondrial

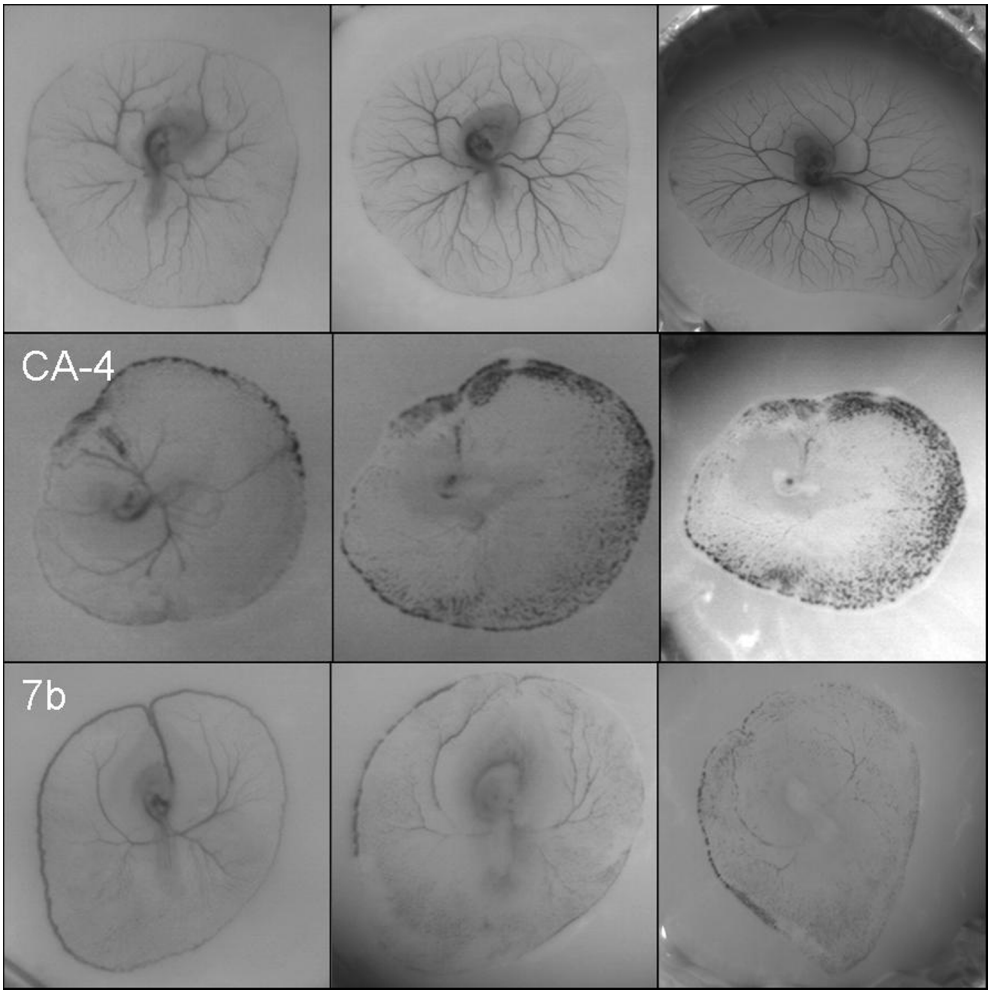


**Figure 4.** Chicken embryos with surrounding blood vessels immediately after adding combretastatin A-4 (CA-4) or **7b** (left), after 1 day (middle), and after 3 days (right). The top row shows a negative control. Pictures are representative of at least two independent runs.

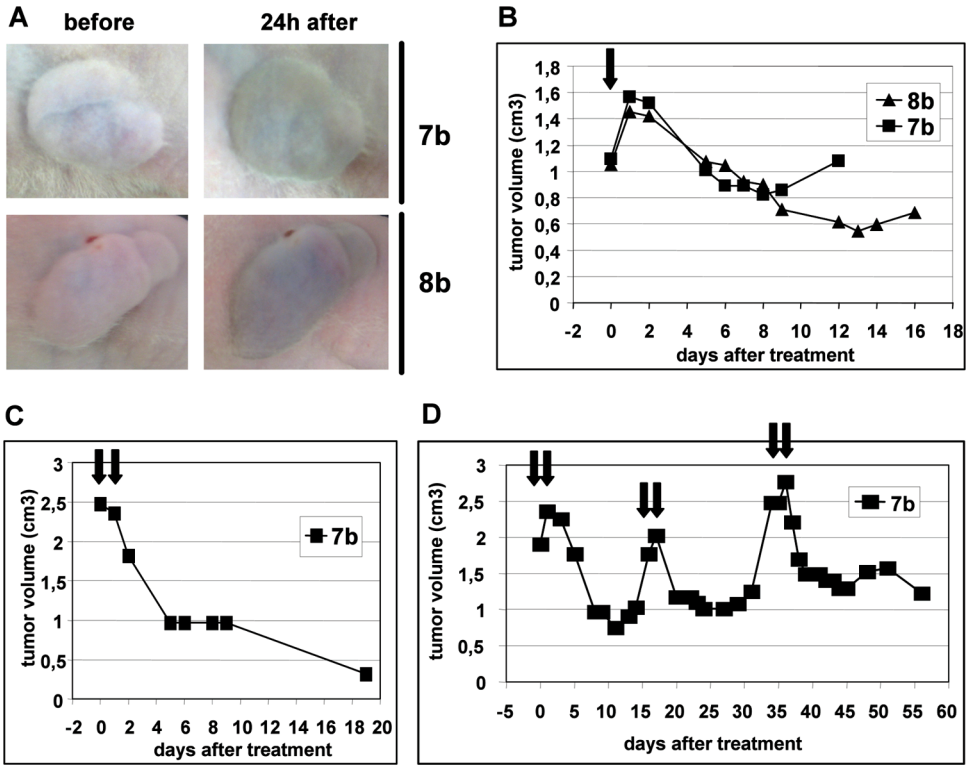


**Figure 5.** In vivo effects of **7b** and **8b** in mouse xenografts of germ cell tumor cell line 1411HP: intratumoral hemorrhage 24 h after treatment (A); tumor response following single-dose (B) and dual-dose (C) applications; tumor response to repeated applications (D). Arrows indicate administration of compounds.

membrane potential.[22] Only ~60% of the mitochondria were intact after incubation with the more cytotoxic compounds **7b**−**d**, **8b**−**d**, and **10a**/**e**, while treatment with **1** left 74% of the mitochondria unaffected. The involvement of reactive oxygen species in the apoptosis of treated HL-60 cells was assessed with the colorimetric nitro blue tetrazolium (NBT) assay but found to be insignificant (cf. Supporting Information).

The most promising of the new oxazoles and imidazoles were tested for antiangiogenic and vasculature disrupting properties using the CAM assay. In this test the vascular system of a fertilized chicken embryo is used as a model.[23] Figure 4 depicts the effects of combretastatin A-4 and **7b** on the development of embryonal blood vessels compared to a negative control (PBS). Both led to a dramatic vessel shrinkage within 24 h after treatment and to a complete degradation of the vascular system within 3 days. Interestingly, the bromo analogue **8b** displayed virtually no effect on this regular embryonal vasculature, which highlights the pivotal role of the halogen substituent. The halogen-free oxazole **10a** also showed no significant antiangiogenic effect.

We then evaluated **7b** and **8b** in mouse xenografts of germ cell tumor cell line 1411HP. Two mice bearing tumors of ~1 $cm^3$ volume were treated with a single dose of 30 mg/kg body weight of **7b** or **8b** which caused transient swelling and strong hemorrhages in the tumors visible after 24 h as a red-blue to brown coloring (Figure 5A). Eventual regression and slow regrowth was observed (Figure 5B). Both mice tolerated this treatment very well. Two mice with xenografts of ~2.5 $cm^3$ volume were administered 20 mg/kg body weight of **7b** on 2 consecutive days. The resulting dramatic regressions, leading even to a stabilization in one case, are shown in Figure 5C,D. The other xenograft regrew and was given two further double doses of **7b** on days 16/17 and 35/36. As shown in Figure 5D, regressions and prolonged periods of stabilization following each application were achieved. Notably, even the third course of treatment was tolerated well and the mouse had regained its original body weight by this time (cf. Supporting Information). These preliminary data demonstrate the potential of **7b** and **8b** for the treatment of resistant tumors.

## Conclusions

The new *N*-methyl-4-(3-halo-4,5-dimethoxyphenyl)-5-(3-amino-4-methoxyphenyl)imidazoles **7b** and **8b** combine chemical stability, good water solubility, and low general toxicity in mice with excellent antitumoral efficacy against various cancer cell lines in vitro, including multidrug-resistant ones, and against certain chemoresistant tumor xenografts in mice. The nature of the halogen substituent is crucial for the selectivity and the magnitude of their bioactivity. Unlike its chloro congener **7b**, the bromoimidazole **8b** was vascular disrupting in tumor xenografts while leaving regular vasculature in chicken embryos (CAM assay) alone. The new imidazoles are also strong inducers of cancer cell apoptosis. Their properties warrant further in vivo evaluations in order to fully elucidate their mode of action and to establish optimized treatment schedules including combinations with other chemotherapeutic agents.

## Experimental Section

**Chemistry.** All starting compounds and combretastatin A-4 were purchased from Aldrich. Compound **1** was prepared according to literature.[11] For chromatography Merck silica gel 60 (230−400 mesh) was used. The following instruments

were used: melting points (uncorrected), Gallenkamp; IR spectra, Perkin-Elmer Spectrum One FT-IR spectrophotometer with ATR sampling unit; nuclear magnetic resonance spectra, BRUKER Avance 300 spectrometer; chemical shifts are given in parts per million ($\delta$) downfield from tetramethylsilane as internal standard; mass spectra, Varian MAT 311A (EI); microanalyses, Perkin-Elmer 2400 CHN elemental analyzer. All tested compounds are >95% pure by elemental analysis.

***N*-[(Toluene-4-sulfonyl)-(3-chloro-4,5-dimethoxyphenyl)methyl]-formamide (5a): Typical Procedure.** 5-Chloroveratraldehyde (5.67 g, 23.44 mmol), *p*-toluenesulfinic acid (3.01 g, 19.29 mmol), and camphorsulfonic acid (110 mg, 0.47 mmol) were treated with formamide (10 mL). Upon heating to 65 °C, the reaction mixture turned into a solution, and after 2 h the product began to precipitate. After the mixture was stirred for 16 h, the precipitate was filtered, washed with methanol, and dried in vacuum. Yield: 4.57 g (11.92 mmol, 51%); colorless solid of mp 157−158 °C; $\nu_{max}$ (ATR)/cm$^{-1}$ 3190, 3107, 2947, 1690, 1593, 1576, 1484, 1470, 1423, 1403, 1308, 1283, 1250, 1215, 1143, 1121, 1078, 1053, 999, 860, 822, 788, 769, 659, 689; $^1$H NMR (300 MHz, DMSO-$d_6$) $\delta$ 2.41 (3 H, s), 3.76 (3 H, s), 3.79 (3 H, s), 6.45 (1 H, d, $J$ = 10.7 Hz), 7.24 (1 H, d, $J$ = 1.9 Hz), 7.30 (1 H, d, $J$ = 1.9 Hz), 7.43 (1 H, d, $J$ = 8.4 Hz), 7.72 (2 H, d, $J$ = 8.4 Hz), 7.98 (1 H, s), 9.74 (1 H, d, $J$ = 10.7 Hz); $^{13}$C NMR (75.5 MHz, $CDCl_3$) $\delta$ 21.1, 56.3, 60.3, 69.5, 113.5, 122.4, 126.7, 127.1, 129.2, 129.6, 133.2, 144.9, 145.4, 153.1, 160.2; *m*/*z* (EI) 382 (4), 278 (6), 227 (89), 192 (76), 156 (57), 113 (55), 91 (100), 77 (67), 63 (92).

**3-Chloro-4,5-dimethoxyphenyl(tosyl)methyl Isocyanide (6a): Typical Procedure.** Formamide **5a** (4.57 g, 11.92 mmol) was suspended in dry DME (100 mL) and cooled to −10 °C. $POCl_3$ (3.4 mL, 36.1 mmol) was added, and a mixture of $Et_3N$ (8.3 mL, 59.5 mmol) in DME (10 mL) was dropped slowly to the reaction mixture. After being stirred for 2 h at −5 °C, the reaction mixture was poured into ice−water. The water phase was extracted with ethyl acetate, and the organic phase was washed with saturated aqueous $NaHCO_3$ and brine, dried over $Na_2SO_4$, filtered, and concentrated in vacuum. By refrigeration overnight a yellow solid crystallized from the residue, which was collected and dried in vacuum. Yield: 2.48 g (6.79 mmol, 57%); yellow solid of mp 115 °C; $\nu_{max}$ (ATR)/cm$^{-1}$ 2920, 2136, 1593, 1577, 1492, 1452, 1423, 1325, 1294, 1276, 1238, 1199, 1137, 1082, 1053, 1002, 862, 826, 759, 705, 683; $^1$H NMR (300 MHz, $CDCl_3$) $\delta$ 2.45 (3 H, s), 3.79 (3 H, s), 3.87 (3 H, s), 5.49 (1 H, s), 6.76 (1 H, d, $J$ = 2.1 Hz), 6.88 (1 H, d, $J$ = 2.1 Hz), 7.34 (2 H, d, $J$ = 8.5 Hz), 7.64 (2 H, d, $J$ 8.5 = Hz); $^{13}$C NMR (75.5 MHz, $CDCl_3$) $\delta$ 21.7, 56.2, 60.8, 75.6, 110.8, 122.2, 122.6, 128.6, 129.9, 130.0, 130.4, 146.9, 147.4, 153.8, 166.6; *m*/*z* (EI) 365 (2) [M$^+$], 278 (7), 246 (10), 210 (100), 155 (23), 91 (54), 66 (20).

**1-Methyl-4-(3′-chloro-4′,5′-dimethoxyphenyl)-5-(4″-methoxy-3″-nitrophenyl)imidazole (7a): Typical Procedure.** A mixture of 4-methoxy-3-nitrobenzaldehyde (76 mg, 0.42 mmol) and 33% $MeNH_2$/ethanol (260 $\mu$L, 2.10 mmol) in ethanol (15 mL) was treated with AcOH (150 $\mu$L) and refluxed for 2 h. After the mixture was cooled down to room temperature, compound **6a** (153 mg, 0.42 mmol) dissolved in DME (10 mL) and $K_2CO_3$ (500 mg, 3.62 mmol) were added. The reaction mixture was refluxed for 3 h. The solvent was evaporated and the residue diluted with ethyl acetate, washed with water and brine, dried over $Na_2SO_4$, filtered, and concentrated in vacuum. The residue was purified by column chromatography (silica gel 60). Yield: 110 mg (0.26 mmol, 62%); yellow oil; $R_f$ = 0.24 (ethyl acetate/methanol 95:5); $\nu_{max}$ (ATR)/cm$^{-1}$ 2939, 1623, 1600, 1566, 1524, 1505, 1483, 1461, 1396, 1342, 1325, 1263, 1230, 1189, 1167, 1112, 1086, 1047, 994, 889, 873, 863, 828, 816, 762, 737, 698, 675; $^1$H NMR (300 MHz, $CDCl_3$) $\delta$ 3.44 (3 H, s), 3.64 (3 H, s), 3.75 (3 H, s), 3.95 (3 H, s), 6.9−7.0 (2 H, m), 7.15 (1 H, d, $J$ = 8.7 Hz), 7.45 (1 H, dd, $J$ = 8.7 Hz, $J$ = 2.2 Hz), 7.50 (1 H, s), 7.78 (1 H, d, $J$ = 2.2 Hz); $^{13}$C NMR (75.5 MHz, $CDCl_3$) $\delta$ 32.1, 55.7, 56.6, 60.5, 109.2, 114.2, 119.7, 122.2, 126.0, 127.3, 127.9, 130.6, 136.4, 137.5, 137.8, 139.7, 144.0, 152.9, 153.4; *m*/*z* (EI) 407 (42), 406 (46), 405 (87) [M$^+$], 404 (77), 403 (100) [M$^+$], 391 (23), 390 (71), 389 (62), 388 (87), 341 (58), 313 (58), 206 (33), 164 (26).

**1-Methyl-5-(3″-amino-4″-methoxyphenyl)-4-(3′-chloro-4′,5′-dimethoxyphenyl)imidazole Bis(hydrochloride) (7b·2HCl): Typical Procedure.** Compound **7a** (109 mg, 0.27 mmol) was dissolved in THF (7.5 mL). Zn powder (107 mg, 1.36 mmol) was added followed by a mixture of concentrated HCl (230 $\mu$L) in THF (1 mL). After being stirred for 15 min at room temperature, the reaction mixture was poured into water and treated with aqueous $NaHCO_3$ to adopt pH 8. The water phase was extracted with ethyl acetate, and the organic phase was dried over $Na_2SO_4$, filtered. The filtrate was concentrated in vacuum. The residue was purified by column chromatography (silica gel 60, 5% methanol/ethyl acetate, $R_f$ = 0.66), giving crude **7b**. This crude product was dissolved in DCM (5 mL) and treated with 3 M HCl/dioxane (1 mL). After the mixture was stirred for 15 min, the solvent was removed and the oily residue was recrystallized from an ethanol/*n*-hexane mixture giving the bis(hydrochloride) salt of **7b**. Yield: 42 mg (0.095 mmol, 40%); colorless solid of mp 180−183 °C; UV (MeOH) $\lambda_{max}$ ($\varepsilon$) 255 (14940). Anal. ($C_{19}H_{22}Cl_3N_3O_3$) C, H, N. $\nu_{max}$ (ATR)/cm$^{-1}$ 3009, 2781, 2578, 1635, 1552, 1517, 1497, 1445, 1409, 1304, 1271, 1147, 1113, 1047, 1025, 998, 830, 762, 739, 721; $^1$H NMR (300 MHz, DMSO-$d_6$) $\delta$ 3.63 (3 H, s), 3.69 (3 H, s), 3.75 (3 H, s), 3.92 (3 H, s), 7.08 (1 H, d, $J$ = 2.1 Hz), 7.16 (1 H, d, $J$ = 2.1 Hz), 9.36 (1 H, s), 7.2−7.4 (3 H, m); $^{13}$C NMR (75.5 MHz, DMSO-$d_6$) $\delta$ 33.9, 56.1, 56.2, 60.4, 110.7, 112.4, 117.6, 119.6, 123.6, 127.3, 127.6, 129.7, 135.7, 145.0, 153.5; *m*/*z* (EI) 375 (20) [M$^+$], 374 (15), 373 (54) [M$^+$], 358 (25), 296 (15), 252 (25), 237 (16), 70 (14), 61 (23), 43 (100).

**Biological Studies. 1. Cell Lines and Culture Conditions.** The HL-60 cells were obtained from the German Collection of Biological Material (DSMZ), Braunschweig, Germany. The human 518A2 melanoma cells and the testicular germ cell tumor cell lines H12.1 and 1411HP were cultured in the Department of Oncology and Hematology, Medical Faculty of the Martin Luther University, Halle, Germany. The KB-V1/Vbl and the MCF-7/Topo cells were obtained from the Institute of Pharmacy of the University Regensburg, Germany, and the colon HT-29 cells from the University Hospital Erlangen, Germany. The HL-60 and the HT-29 cells were grown in RPMI-1640 medium supplemented with 10% fetal calf serum (FCS), 100 IU/mL penicillin G, 100 $\mu$g/mL streptomycin sulfate, 0.25 $\mu$g/mL amphotericin B, and 250 $\mu$g/mL gentamycine (all from Gibco, Egenstein, Germany). The 518A2 and the KB-V1/Vbl cells were cultured in Dulbecco's modified Eagle medium (D-MEM, Gibco) containing 10% FCS, 100 IU/mL penicillin G, 100 $\mu$g/mL streptomycin sulfate, 0,25 $\mu$g/mL amphotericin B, and 250 $\mu$g/mL gentamycine. The MCF-7/Topo cells were grown in E-MEM medium (Sigma) supplemented with 2.2 g/L $NaHCO_3$, 110 mg/L sodium pyruvate, and 5% FCS. The cells were maintained in a moisture-saturated atmosphere (5% $CO_2$) at 37 °C in 75-mL culture flasks (Nunc, Wiesbaden, Germany). They were serially passaged following trypsinization by 0.05% trypsin/0.02% EDTA (PAA Laboratories, Cölbe, Germany). Mycoplasma contamination was routinely monitored, and only mycoplasma-free cultures were used.

**2. Determination of Tumor Cell Growth (MTT Assay).** MTT [3-(4,5-dimethylthiazol-2-yl)-2,5-diphenyltetrazolium bromide] (ABCR) was used to identify viable cells that reduce it to a violet formazan.[24] HL-60 leukemia cells ($5 \times 10^5$/mL) and cells ($5 \times 10^4$/mL) of 518A2 melanoma, HT-29 colon, KB-V1/Vbl cervix, and MCF-7/Topo breast carcinoma were seeded out in 96-well tissue culture plates and cultured for 24 h. Incubation (5% $CO_2$, 95% humidity, 37 °C) of the cells following treatment with the test compounds was continued for 24, 48, or 72 h. Blank and solvent controls were treated identically. MTT in phosphate buffered saline (5 mg/mL) was added to a final concentration of 0.05% (HL-60, 518A2) or 0.1% (HT-29, KB-V1/Vbl, MCF-7/Topo). After 2 h the formazan precipitate was dissolved in 10% sodium dodecyl sulfate in DMSO containing 0.6% acetic acid in

the case of the HL-60 cells. For the adherent 518A2, KB-V1/Vbl, MCF-7/Topo, and HT-29 cells the microplates were swiftly turned to discard the medium before adding the solvent mixture. The microplates were gently shaken in the dark for 30 min, and absorbance at 570 and 630 nm (background) was measured with an ELISA plate reader. All experiments were carried out in quadruplicate. The percentage of viable cells was calculated as the mean ± SD with controls set to 100%.

**3. CAM Assay.** Fertilized chicken eggs received from a nearby farm directly after laying have been incubated at 36−38 °C and a relative humidity of 60%. During the growth the eggs have been held in an inclined position and turned from time to time in order to avoid an adherence to the shell. After 4 days each embryo was transferred into a cavity created by fixing a thin plastic foil on top of a cup and covered. This was done by opening the shell at the flat end where the air sac resides and letting the content slip out. There the growth continued for another 2−4 days until the first blood vessels became visible. Then an amount of 10 nmol of the substance to be tested (in 10 μL PBS with 1% DMF) was applied directly on the embryonal vessels. As a reference, PBS was used. Finally incubation continued for up to another 3 days.[25,26]

**4. SRB Cytotoxicity Assay.** Dose-response curves of the testicular germ cell tumor cell lines exposed to drug concentrations of 0.001−10 μM were established using the sulforhodamine B (SRB) microculture colorimetric assay[27] and performed as previously described.[21] Briefly, cells were seeded into 96-well plates on day 0 at cell densities previously determined to ensure exponential cell growth during the period of the experiment. On day 1, cells were treated with the drugs dissolved in medium to give the appropriate concentrations for indicated times, and the percentage of surviving cells relative to untreated controls was determined on day 5.

**5. Tubulin Polymerization Assay.** Analysis of tubulin polymerization was performed using the tubulin polymerization assay kit (Cytoskeleton) according to manufactures instructions. The assay is fluorescence-based, and tubulin polymerization was followed by measuring RFU (relative fluorescence units) on the SpectraFluorPlus (Tecan, Switzerland) using the following filters: excitation 360 nm, emission 465 nm.

**6. Animal Studies.** In vivo antitumor activity and tolerability of compounds were studied in a nude mouse xenograft model of the resistant germ cell tumor cell line 1411HP employing Athymic Nude-Fox n1 nu/nu mice (Harlan und Winkelmann, Borchen, Germany). They were kept under pathogen-free conditions, fed on an autoclaved standard diet, and given free access to sterilized water. The study had been approved by the Laboratory Animal Care Committee of Sachsen-Anhalt, Germany. Each of five mice was administered a 150 μL PBS suspension of 10 million 1411HP cells into the left flank to generate subcutaneous xenograft tumors. After 4 weeks one group of two mice bearing 1411HP xenografts with a volume of ∼1 $cm^3$ was injected ip with a single dose of 30 mg/kg body weight of **7b** or **8b**, respectively. Two mice in the second group with xenografts of a volume of ∼2.5 $cm^3$ were injected ip with 20 mg/kg body weight of **7b** on 2 consecutive days. Tumor volumes were calculated by caliper measurement using the formula $a^2 \times b \times 0.5$ with $a$ being the short dimension and $b$ the long dimension. Body weight was assessed twice weekly and daily while under therapy.

**Acknowledgment.** This work was supported by a grant from the Deutsche Forschungsgemeinschaft (Grant Scho 402/8-3). We thank Franziska Reipsch for her excellent technical assistance.

**Supporting Information Available:** Syntheses and characterization of derivatives **4**−**5b**/**c**, **7c**/**d**, **8a**−**d**, **9**, **10**; MTT and SRB assays; TUNEL assays with HL-60 cells; ROS generation and effects on mitochondria; in vivo body weight−time curves; maximal slopes of tubulin polymerization curves. This material is available free of charge via the Internet at http://pubs.acs.org.

## References

(1) Pettit, G. R.; Singh, S. B.; Hamel, E.; Lin, C. M.; Alberts, D. S.; D. Garcia-Kendall, D. Isolation and structure of the strong cell growth and tubulin inhibitor combretastatin A-4. *Experientia* **1989**, *45*, 209–211.

(2) Mooney, C. J.; Nagaiah, G.; Fu, P.; Wasman, J. K.; Cooney, M. M.; Savvides, P. S.; Bokar, J. A.; Dowlati, A.; Wang, D.; Agarwala, S. S.; Flick, S. M.; Hartman, P. H.; Ortiz, J. D.; Lavertu, P. N.; Remick, S. C. A phase II trial of fosbretabulin in advanced anaplastic thyroid carcinoma and correlation of baseline serum-soluble intracellular adhesion molecule-1 with outcome. *Thyroid* **2009**, *19*, 233–240.

(3) Rustin, G. J.; Shreeves, G.; Nathan, P. D.; Gaja, A.; Ganesan, T. S.; Wang, D.; Boxall, J.; Poupard, L.; Chaplin, D. J.; Straford, M. R. L.; Balkissoon, J.; Zweifel, M. A phase Ib trial of CA4P (combretastatin A-4 phosphate), carboplatin, and paclitaxel in patients with advanced cancer. *Br. J. Cancer* **2010**, *102*, 1355–1360.

(4) Tron, G. C.; Pirali, T.; Sorba, G.; Pagliai, F.; Busacca, S.; Genazzani, A. A. Medicinal chemistry of combretastatin A4: present and future directions. *J. Med. Chem.* **2006**, *49*, 3033–3044.

(5) Wankhede, M.; Dedeugd, C.; Siemann, D. W.; Sorg, B. S. In vivo functional differences in microvascular response of 4T1 and Caki-1 tumors after treatment with OXi4503. *Oncol. Rep.* **2010**, *23*, 685–692.

(6) Holwell, S. E.; Cooper, P. A.; Thompson, M. J.; Pettit, G. R.; Lippert, J. W.; Martin, S. W.; Bibby, M. C. Anti-tumor and anti-vascular effects of the novel tubulin-binding agent combretastatin A-1 phosphate. *Anticancer Res.* **2002**, *22*, 3933–40.

(7) Madlambayan, G. J.; Meacham, A.; Hosaka, K.; Mir, S.; Jorgensen, M.; Scott, E. W.; Siemann, D. W.; Cogle, C. R. Leukemia regression by vascular disruption and anti-angiogenic therapy. *Blood* [Online early access]. DOI: 10.1182/blood-2009-06-230474. Published Online: May 14, 2010.

(8) Dalal, S.; Burchill, S. A. Preclinical evaluation of vascular-disrupting agents in Ewing's sarcoma family of tumours. *Eur. J. Cancer* **2009**, *45*, 713–722.

(9) Folkes, L. K.; Christlieb, M.; Madej, M.; Stratford, M. R. L.; Wardman, P. Oxidative metabolism of combretastatin A-1 produces quinone intermediates with the potential to bind to nucleophiles and to enhance oxidative stress via free radicals. *Chem. Res. Toxicol.* **2007**, *20*, 1885–1894.

(10) Pettit, G. R.; Thornhill, A. J.; Moser, B. R.; Hogan, F. Antineoplastic agents. 552. Oxidation of combretastatin A-1: trapping the *o*-quinone intermediate considered the metabolic product of the corresponding phosphate prodrug. *J. Nat. Prod.* **2008**, *71*, 1561–1563.

(11) Wang, L.; Woods, K. W.; Li, Q.; Barr, K. J.; McCroskey, R. W.; Hannick, S. M.; Gherke, L.; Credo, R. B.; Hui, Y.-H.; Marsh, K.; Warner, R.; Lee, J. Y.; Zielinski-Mozng, N.; Frost, D.; Rosenberg, S. H.; Sham, H. L. Potent, orally active heterocycle-based combretastatin A-4 analogues: synthesis structure−activity relationship, pharmacokinetics, and in vivo antitumor activity evaluation. *J. Med. Chem.* **2002**, *45*, 1697–1711.

(12) Pettit, G. R.; Toki, B. E.; Herald, D. L.; Boyd, M. R.; Hamel, E.; Pettit, R. K.; Chapuis, J.-C. Antineoplastic agents. 410. Asymmetric hydroxylation of trans-combretastatin A-4. *J. Med. Chem.* **1999**, *42*, 1459–1465.

(13) Pettit, G. R.; Rhodes, M. R.; Herald, D. L.; Chaplin, D. J.; Stratford, M. R. L.; Hamel, E.; Pettit, R. K.; Chapuis, J.-C.; Oliva, D. Antineoplastic agents. 393. Synthesis of the trans isomer of combretastatin A-4 prodrug. *Anti-Cancer Drug Des.* **1998**, *13*, 981–993.

(14) Brown, T.; Holt, H., Jr.; Lee, M. Synthesis of biologically active heterocyclic stilbene and chalcone analogs of combretastatin. *Top. Heterocycl. Chem.* **2006**, *2*, 1–51.

(15) Pettit, G. R.; Minardi, M. D.; Rosenberg, H. J.; Hamel, E.; Bibby, M. C.; Martin, S. W.; Jung, M. K.; Pettit, R. K.; Cuthbertson, T. J.; Chapuis, J.-C. Antineoplastic agents. 509. Synthesis of fluorcombstatin phosphate and related 3-halostilbenes. *J. Nat. Prod.* **2005**, *68*, 1450–1458.

(16) Hall, J. J.; Sriram, M.; Strecker, T. E.; Tidmore, J. K.; Jelinek, C. J.; Kumar, G. D. K.; Hadimani, M. B.; Pettit, G. R.; Chaplin, D. J.; Trawick, M. L.; Pinney, K. G. Design, synthesis, biochemical, and biological evaluation of nitrogen-containing trifluoro structural modifications of combretastatin A-4. *Bioorg. Med. Chem. Lett.* **2008**, *18*, 5146–5149.

(17) Lawrence, N. J.; Rennison, D.; Hadfield, J.; McGown, A. T. Synthesis and anticancer activity of fluorinated combretastatins. *Abstr. Pap.—Am. Chem. Soc.* **2003**, *226*, U523–U523.
(18) Lawrence, N. J.; Hepworth, L. A.; Rennison, D.; McGown, A. T.; Hadfield, J. A. Synthesis and anticancer activity of fluorinated analogues of combretastatin A-4. *J. Fluorine Chem.* **2003**, *123*, 101–108.
(19) Bailey, K.; Tan, E. W. Synthesis and evaluation of bifunctional nitrocatechol inhibitors of pig liver catechol-*O*-methyltransferase. *Bioorg. Med. Chem.* **2005**, *13*, 5740–5749.
(20) Andrew, R. G.; Raphael, R. A. A new total synthesis of aaptamine. *Tetrahedron* **1987**, *43*, 4803–4816.
(21) Müller, T.; Voigt, W.; Simon, H.; Frühauf, A.; Bulankin, A.; Grothey, A.; Schmoll, H.-J. Failure of activation of caspase-9 induces a higher threshold for apoptosis and cisplatin resistance in testicular cancer. *Cancer Res.* **2003**, *63*, 513–521.
(22) Desager, S.; Osen-Sand, A.; Nicholas, A.; Eskes, R.; Montessuit, S. Bid-induced conformational change of Bax is responsible for mitochondrial cytochrome c release. *J. Cell Biol.* **1999**, *144*, 891–901.
(23) Wilting, J.; Christ, B.; Bokeloh, M. A modified chorioallantoic membrane (CAM) assay for qualitative and quantitative study of growth factors. Studies on the effects of carriers, PBS, angiogenin, and bFGF. *Anat. Embryol.* **1991**, *183*, 259–271.
(24) Mosmann, T. Rapid colorimetric assay for cellular growth and survival: application to proliferation and cytotoxicity assays. *J. Immunol. Methods* **1983**, *65*, 55–63.
(25) Dugan, J. D., Jr.; Lawton, M. T.; Glaser, B.; Brem, H. A new technique for explantation and in vitro cultivation of chicken embryos. *Anat. Rec.* **1991**, *229*, 125–128.
(26) Fisher, C. J. Chick embryos in shell-less culture. *Tested Stud. Lab. Teach.* **1993**, *5*, 105–115.
(27) Papazisis, K. T.; Geromichalos, G. D.; Dimitriadis, K. A.; Kortsaris, A. H. Optimization of the sulforhodamine B colorimetric assay. *J. Immunol. Methods* **1997**, *208*, 151–158.